PHYSICAL REVIEW B VOLUME 51, NUMBER 3 15 JANUARY 1995-I

Alkali-metal chemisorption on Ta(110)

E. Kneedler, A. B. Andrews, Won-Kook Choi, and S. D. Kevan
Department of Physics, University of Oregon, Eugene, Oregon 97403

(Received 9 May 1994; revised manuscript received 19 September 1994)

The effect of alkali-metal chemisorption on the surface electronic structure of Ta(110) is presented. A *d*-derived surface state on clean Ta(110) is strongly modified, as manifested by a level shift and lateral delocalization. Strong mixing between alkali-metal and substrate valence bands is observed. It is suggested that alkali-metal overlayers on the more complex metals have fundamentally different behavior than on simple metal substrates.

INTRODUCTION

The chemisorption of alkalis on metals has received much attention for some time, particularly in recent years. There are several reasons for this. From a practical standpoint, alkalis have long been known to affect surface processes, including catalytic promotion and enhancement of photoreceptivity. More fundamentally, the monovalent alkalis are a relatively simple adatom in ordinarily complicated systems of chemisorption. Perturbation via alkation will help determine how a known clean surface interacts with its environment. Furthermore, alkali overlayers provide a setting for studying two-dimensional (2D) electronic states, especially if interaction with the substrate can be separated from intralayer dynamics.

Historically, alkali/metal behavior has been described in terms of the work function behavior, a macroscopic representation of the redistribution of surface charge. For all alkali/metal systems, the work-function energy initially undergoes a negative linear shift as a function of coverage, but eventually reaches a saturation at 1 ML after passing through a minimum. This fostered hope that a unifying model of alkalis/metals was feasible. The conventional model involves the donation of the alkali *ns* valence electron to the substrate, resulting in an ionic bond. At sufficiently low coverage, the net dipole of the adsorbed layer is the sum of individual dipoles, hence the linear work-function behavior. At higher coverages, adatom-adatom dipole interaction results in depolarization, which is eventually sufficient to produce the characteristic minimum, then saturation of the work function. The macroscopic nature of the work function apparently permits such a simple description. However, a microscopic treatment is necessary not only for a more fundamental understanding of the work function, but also for an accurate explanation of the other aspects of alkali overlayers mentioned above.

The first quantum-mechanical treatment of the problem was by Gurney.[1] In this model, the alkali atomic *ns* level, initially centered well above the substrate Fermi level E_F, is broadened when brought near enough to interact with the substrate continuum. Charge transfer to the substrate is still key to this approach, although the transfer is generally incomplete. The ionicity is defined by the degree of the *ns*-resonance occupation. As the work function is lowered, so is the energy of the alkali *ns* resonance. As more of the resonance is occupied, the polarization is reduced, thus giving the required work-function behavior. A critical assumption of the Gurney model is that the details of the substrate electronic structure are unimportant, an idea which persisted in more refined calculations.[2,3] In particular, hybridization between the alkali valence bands and the transition-metal substrate *d* bands was neglected.[3] This seemed reasonable because of similar work-function behavior for alkalis on very different metal substrates, and the work-function behavior could be accurately predicted. However, a large variety of recent experiments measuring electronic structure and overlayer structure have revealed significant differences for alkalis on different substrates.

It has been shown that for the Al(100) substrate, the charge-transfer model is reasonably accurate in the limit of an isolated adatom, provided screening effects in the substrate are considered.[4] In this limit, this is thought to be generally useful for other substrates. However, for the low-coverage regime between infinitesimal coverage and the generally metallic high (but submonolayer) coverage regime, the usefulness of the Gurney model is still a matter of debate. The observation[5–9] and subsequent modeling[10] of a discontinuity in the occupation of the alkali *ns* level with coverage has lead to a discussion of the transition to metallicity. The Gurney model predicts no such discontinuities. As yet, sharp alkali overlayer transitions have been observed only on simpler metal substrates, and are usually associated with overlayer condensation. Meanwhile, the Gurney model has been dismissed for several transition-metal substrates, in favor of a "polarized covalent" picture. These systems, complicated by hybridization of the alkali valence and substrate *d* bands, may be rather different than simpler metal substrates. In particular, it seems that abrupt transitions to metallicity are not a common characteristic of alkalis on transition metals.

A signature of metallicity is the delocalization of electronic states at the Fermi level. An insulator-metal transition generally involves the appearance of partially occupied delocalized bands, replacing the localized atomiclike levels characteristic of the noninteracting low-density limit. For a Mott transition, the onset of metallicity occurs when the overlap interaction is sufficient to overcome localizing correlation effects.[11] The 2D transitions mentioned above are not truly Mott transitions because of the presence of the substrate and because of disorder in the adsorbed layer. The charge transfer at lower coverage permits a delocalized band to be essentially unoccupied, and the transition to metallicity instead occurs when the band is shifted to the Fermi level. Discussions about the transition thus usually revolve around the energy and width of the alkali *ns* band as a function of coverage. Implicit is the assumption that alkali valence bands can be distinguished from substrate electronic structure.

It has been suggested that the magnitude of the adatom-substrate interaction relative to the adatom-adatom interaction is of critical importance to overlayer behavior.[12,13] The fact that sharp alkali nonmetal-metal transitions have been observed only on substrates which have relatively weak alkali-substrate interactions supports this notion. On the other hand, alkali atoms interact strongly with metal surfaces, such as the (100) faces of W, Mo, and Ta.[14–16] Hybridization of alkali and substrate bands could certainly affect the behavior of the alkali *ns* band. Unfortunately, the complexity of *d*-band metals tends to make interpretation of data ambiguous due to overlap between the alkali *s* and substrate *d* bands. The relative simplicity of the Ta(110) surface valence electronic structure minimizes, but does not eliminate, these difficulties. The alkali overlayers on Ta(110) discussed here each exhibit qualitatively different behavior than on simpler metal substrates at all submonolayer coverages. Further, we speculate that the notion of a nonmetal-metal transition in the alkali layer is irrelevant for Ta(110) and similar surfaces.

The Ta(110) surface valence electronic structure has already provided insight into interactions between a surface layer and the bulk.[17] A single clean surface state of even symmetry exists within a projected Ta bulk band gap at zone center, and with increasing $k_{\parallel}$ merges with the bulk continuum edge. This predominantly d_{z^2} state extends deeply into the vacuum, resulting in substantial spatial overlap with adsorbate wave functions. Upon hydrogen chemisorption, the state at zone center shifts nearly 2 eV discontinuously to higher binding energy. The pure state at zone center is dispersionless until near the point where it crosses the edge of the bulk band continuum, for both clean and hydrogen-covered surfaces. The lack of dispersion and the discontinuous shift of the hydrogen-modified surface state indicate that it remains laterally localized. The interaction of the delocalized alkali *ns* levels with the Ta(110) surface state is quite different, and will be contrasted with the hydrogen behavior.

EXPERIMENT

The Ta(110) crystal was cleaned and characterized as described previously.[15] The predominantly oxide contamination was less than 1%. Data were collected at the National Synchrotron Light Source using a 6-m Toroidal Grating Monochromator. Total instrumental resolution was better than 150 meV. Base pressure was $1-2\times10^{-10}$ torr. Alkalis were deposited using SAES getters for Li, Na, K, Rb, and Cs, which were each conditioned for about 1 day to remove impurities. Full coverage was obtained in a few minutes with background pressure rising negligibly. Doses were characterized by measurements of work-function shift ($\Delta\Phi$) which were measured by monitoring the energy of the secondary photoelectron cutoff of a negatively biased sample, and coverage was estimated via calibration with previous experiments.[18,19] As indicated in Table I, we observed for all alkalis a minimum in work function, followed by "saturation" as a function of coverage at monolayer coverage. Most experiments were conducted at or slightly above room temperature. However, Na- and Rb-covered surfaces were also deposited at 160–200 K. At room temperature, monolayer coverage was truly the saturated limit for all alkalis except Li, which apparently could be grown up to 3 ML. Na depos-

TABLE I. Work-function shifts, energy of the modified surface state, and effective masses for monolayers of alkalis and hydrogen on Ta(110). The value of the work function at its minimum and saturated monolayer coverage are shown. The effective masses were measured in the two principal azimuths by fitting parabolas to the data nearest $\bar{\Gamma}$. Note the general asymmetry in effective mass for the two azimuths reflecting substantial hybridization with the substrate. The room-temperature data for Na are anomalous in this regard, since the asymmetry is in the opposite direction than for the other films. Unless otherwise noted, data were collected near room temperature.

Overlayer	$\Delta\phi_{\mathrm{min}}$ (eV)	$\Delta\phi_{\mathrm{sat}}$ (eV)	ML binding energy (eV)	$\frac{m^*_{\bar{\Delta}}}{m_e}$	$\frac{m^*_{\bar{\Sigma}}}{m_e}$
Clean	0.00	0.00	0.47	∞	∞
Li	−2.51	−1.90	2.15	1.69	2.26
Na	−3.05	−2.45	2.15	1.58	1.32
Na[a]	−3.08	−2.37	2.28	1.52	1.86
K	−3.30	−2.65	1.58	1.27	1.69
Rb[a]	−3.5	−2.8	1.51	2.50	2.60
Cs	−3.80	−3.15	1.33	1.47	1.60
H	0.5	0.5	2.4	∞	∞

[a] $T\cong160$ K.

ited at 160–200 K could also be grown up to 3 ML. Full monolayer surfaces were stable for 15 min (Li) to 1.5 h (K and Na) as determined by deterioration of spectra. Stability of fractional coverages was somewhat less. At low temperatures the surfaces were very inert, with identical spectra even after several hours in vacuum. Low-energy electron diffraction (LEED) patterns ranged from fuzzy distorted hexagonal (Na) to a diffuse ring (most other alkalis) superimposed on a sharp Ta(110) pattern, implying a somewhat disordered incommensurate overlayer. No conclusive evidence for a structural phase transition of the overlayer was obtained from LEED.

An exploratory angle-resolved photoelectron (ARP) study for up to 3 ML Li and Na overlayers revealed well-defined states in the projected Ta(110) band gap.[20] These were identified as quantum-well states resulting from the discretization of the alkali bulk bands. The unusually sharp nature of these features suggests that they tunnel only weakly into the substrate. Coverage-dependent behavior indicates islanding layer-by-layer growth.

RESULTS AND DISCUSSION

Na/Ta(110)

The effect on the Ta(110) surface electronic structure of submonolayer Na adsorption is illustrated in the normal emission spectra in Fig. 1. The clean surface state, seen as a large photoemission peak near E_F in the bottom spectrum, is continuously shifted and quenched with increasing coverage. By monolayer coverage, the state has shifted from 0.46 to 2.2 eV binding energy (BE). At higher coverages, a second feature appears just below E_F. The small peak at BE of 1.7 eV is a result of the onset of two-layer growth, and will be ignored until later in this paper. The data in Fig. 1 were taken at room temperature, and are qualitatively similar to data for $T_{\text{sample}} \sim 160$ K. However, at colder temperatures the overlayer is apparently more uniform, leading to sharper spectral features, as shown in Fig. 2. Careful examination of the low-temperature high-coverage spectra show that the second feature apparently shifts from above E_F. At room temperature, this shift cannot be resolved due to the broader peak combined with the proximity to E_F.

Figure 3 shows ARP spectra representing the dispersion of monolayer Na/Ta(110) valence bands along $\bar{\Delta}$ near zone center. The Na-modified surface state, with 2.2-eV BE at the center of the Surface Brillouin zone (SBZ), is well within the Ta(110) projected bulk band gap. There is obvious dispersion with $k_{\parallel}$, uncharacteristic of the clean Ta(110) surface state. As the band reaches the bulk continuum edge, it merges with it, as for the clean surface. The enhanced photoemission intensity at larger $k_{\parallel}$ is due to increased *d*-band character as the state approaches to Ta bulk band. The alkali-induced dispersion is consistent with the intermixing of alkali *ns* electrons. When these data are plotted on the SBZ band map of Fig. 4, it is evident that the dispersion is parabolic in both azimuths for SBZ points within the projected bulk Ta gap.

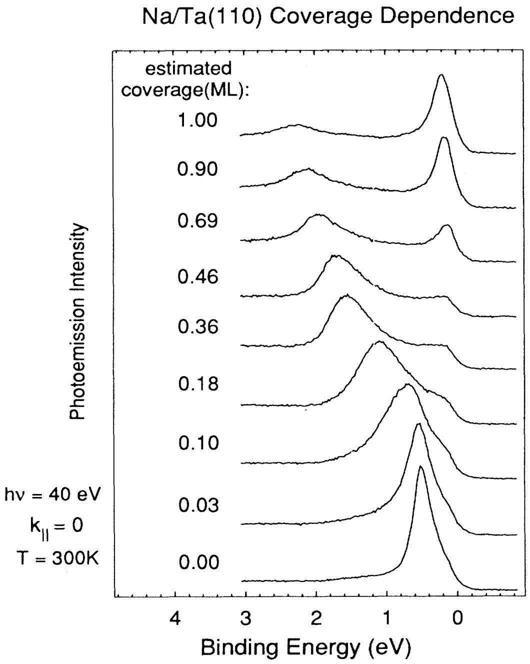

FIG. 1. Normal emission ARP spectra of sodium on Ta(110) as a function of coverage. Spectra were taken at room temperature. The clean Te surface state at BE of 0.46 eV is continuously quenched and shifted to BE of 2.15 eV by monolayer coverage Na. A Na-induced feature appears just below E_F for higher coverages.

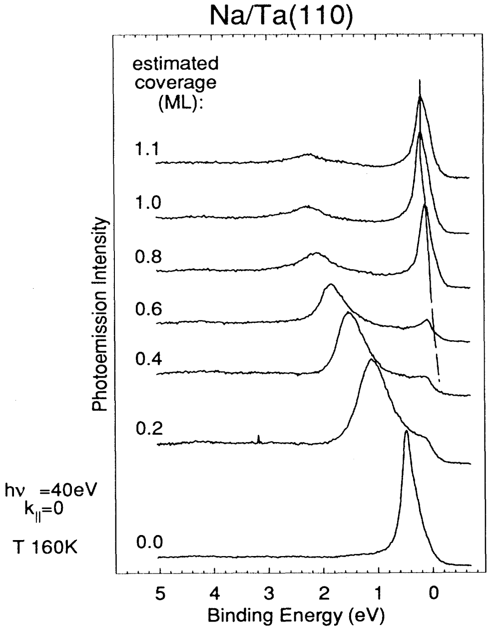

FIG. 2. Normal emission ARP spectra of sodium on Ta(110) as a function of coverage, with sample cooled to $T \sim 160$ K. The clean Ta surface state at BE of 0.46 eV is continuously quenched and shifted to BE of 2.27 eV by monolayer coverage Na. A Na-induced feature disperses below E_F for higher coverages.

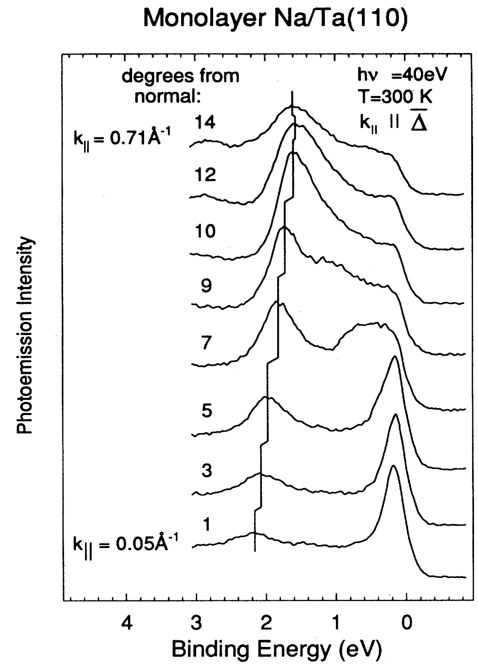

FIG. 3. ARP spectra of 1 ML of Na on Ta(110) as a function of collection angle along the $\bar{\Delta}$ mirror plane. The dispersion of the Na-modified surface state is indicated. Data were collected at room temperature, with a photon energy of 40 eV.

Measurements of intermediate-coverage dispersions show the transition from flat to parabolic behavior to be smooth and monotonic. Figure 5 demonstrates this for Na/Ta(110). The onset of dispersion in the modified Ta surface band can be detected even at very low coverages. This display of Na 3*s* character is important, since for some other systems the alkali *ns* band is presumed unoccupied at low coverage.

Alkali-substrate hybridization

The reduced photoemission intensity, acquired dispersion, and energy shift of the Na-modified surface state suggest that its orbital character has changed substantially. This implies hybridization with an extrinsic level, namely, the Na *ns* valence band. At $h\nu=40$ eV, the photoemission cross section for *d* bands is much larger than for *s* and *p* bands. Thus, the ARP spectra in the previous figures are dominated by *d*-orbital features. If an initially *d*-type feature hybridized with an *s* band, then the extent to which it has *s* character will be reflected as a reduction in photoemission intensity. That the Na-modified state is nearly quenched suggests that it has little *d* character left. The feature observed at higher coverage at E_F, however, must have substantial *d* character. Similarly, the enhanced photoemission intensity of the alkali-shifted surface state at larger $\mathbf{k}_{\parallel}$ is due to increased *d*-band character as the state approaches the Ta bulk band. Also, the initially dispersionless state acquires substantial disper-

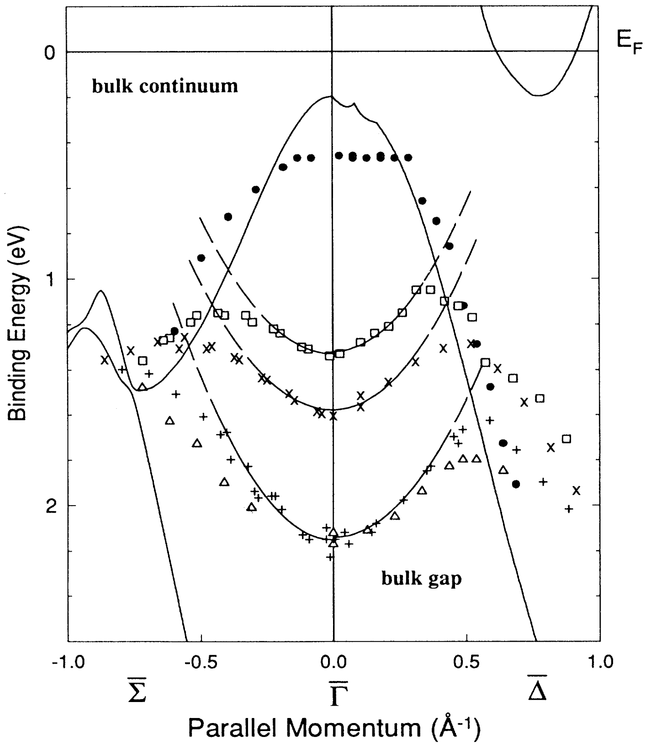

FIG. 4. Summary of single alkali monolayers on Ta(110). The energies of the clean surface state (●) and the Li (△), Na (+), K (×), and Cs (□) alkali-modified states are plotted as a function of $\mathbf{k}_{\parallel}$. Fitted parabolas are shown for Na, K, and Cs.

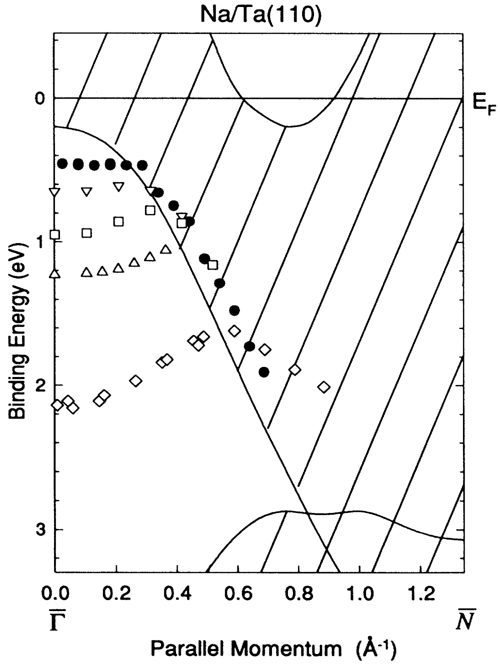

FIG. 5. Coverage-dependent dispersion relations along the $\bar{\Delta}$ mirror plane for sodium on Ta(110). Clean surface state (●) is continuously shifted to higher binding energy as a function of Na coverage. Estimated coverages (in ML) are 0.12 (▽), 0.20 (□), 0.32 (△), and 1.0 (◇). Data were collected at room temperature, with a photon energy of 40 eV.

sion, characteristic of the alkali NFE valence *ns* band. Finally, the energy shift suggests that a covalent interaction may be responsible.

A naive approach to modeling the interaction between the Ta d_{z^2} surface state and the Na *ns* band involves the heterogeneous diatomic covalent bonding model.[21] In this model, the Ta surface state and the Na level are treated as atomic levels. This is not entirely unreasonable in the limit of an isolated adatom, considering the localization of the surface state. The modified surface state is thus interpreted as the bonding level of the initial Ta and Na levels. Of course, a direct measurement of the initial energy of the Na 3*s* level is not possible in this experiment. However, it can be assumed to start above E_F at low coverage, and shift monotonically below E_F at higher coverages. The antibonding level would thus be above E_F at lower coverages. It is likely that the peak in Figs. 1 and 2 just below E_F at higher coverages is essentially the antibonding level, which shifts to lower energy with the Na 3*s* band. However, contributions from bulk Ta electrons, or even from the Na 3*p* level, cannot be ruled out. On simpler substrates, a similar appearance of a photoemission peak at E_F has been interpreted as the onset of a partially occupied alkali *ns* band.[4–6] Our data must be interpreted differently. For the same reason that the bonding level indicates loss of *d* character, the E_F peak in Fig. 1 must have substantial *d* character. The antibonding level would exhibit much of the character of the Ta surface state, which was lost in the bonding level. At room temperature, there is no measurable dispersion of this band at E_F. Except for a small shift towards E_F, the feature is very similar to the Ta clean surface state. Cooling the sample to ~160 K sharpens the features, revealing a slight positive dispersion, shown in Fig. 6. This suggests some intermixing of Na 3*s* (or 3*p*) electrons with the Ta surface state. While this simplistic model is instructive for understanding the nature of the alkali bonding to the substrate, it is important to stress its shortcomings. The surface density of states (DOS) is certainly more complex than the simplified surface state used above. Also, the alkali *ns* state is a 2D band at higher coverages, and is resonant with the Ta bulk bands even in the limit of isolated adatoms. Finally, contributions from other levels, such as the alkali *np* level, may need to be considered. To characterize the bonding, a more elaborate model is needed. A good approach might be to employ the coherent-potential approximation, which is currently the best method to deal with the complicated covalent interactions in random alloys.[22]

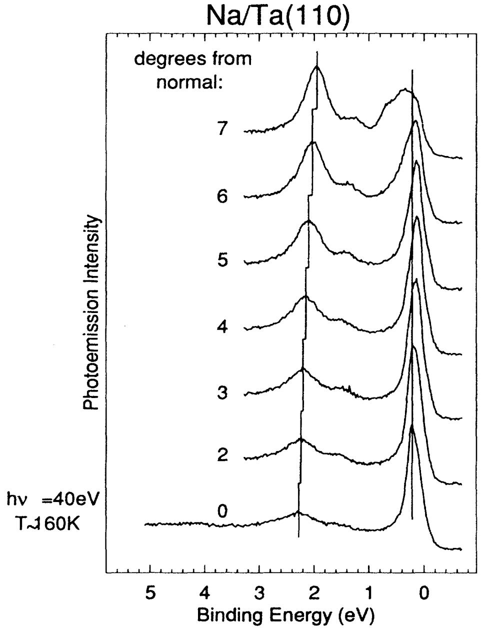

FIG. 6. ARP spectra of 1 ML of Na on Ta(110) as a function of collection angle along the $\bar{\Delta}$ mirror plane near $\bar{\Gamma}$. Sample was cooled to $T \sim 160$ K. The dispersion of the Na-modified surface state is indicated. For comparison, the line at BE of 0.21 eV shows the energy of the peak near E_F at $\bar{\Gamma}$. The top spectrum, at 7° from normal collection angle, is at $k_{\parallel}=0.37$ Å^{-1}.

Other alkalis/Ta(110)

For all alkalis, the chemisorption behavior is qualitatively similar. The $\mathbf{k}_{\parallel}$ dispersions are summarized in Fig. 4. The Rb/Ta(110) data have been omitted for clarity. There is a trend of larger surface state shift for lighter alkali species. Table I summarizes the relative shifts of the work function and surface state, as well as the effective-mass measurements. To determine the effective mass m^* of the alkali-modified state, parabolic least-squares fits were performed for each alkali near the center of the SBZ, in each azimuth independently. Usually 7–10 points were used for each fit, with the obvious deviations from parabolic behavior near the gap edge omitted. Our results are roughly consistent with the corresponding bulk alkali values. There are subtle differences in coverage-dependent behavior for different alkali species. The normal emission spectra for Cs/Ta(110) in Fig. 7 show the clean surface state continuously shifted to higher binding energy as coverage increases, as for Na/Ta(110). For Cs, however, the photoemission intensity is not reduced nearly as much, and the magnitude of the shift is about half that of the Na-modified state. The lower number density of the Cs monolayer, due to a larger atomic radius, probably contributes to this, but the magnitude of the alkali-substrate interaction discussed below must also be considered.

The lateral range of the alkali valence band is evident in the subtle variations in coverage-dependent behavior observed for different alkali types. For the heavier alkalis, there is no appreciable broadening of the modified surface state that cannot be explained by the inverse-hole lifetime. For the lightest alkalis, however, there is significant broadening, especially at low coverage. A comparison of Figs. 1 and 7 illustrates this. This behavior can be understood qualitatively by considering the reduced range but increased strength of the alkali pseudopotential for the lighter alkalis. This also offers an explanation for the variations for different alkalis in level shift and reduction in photoemission intensity. The mag-

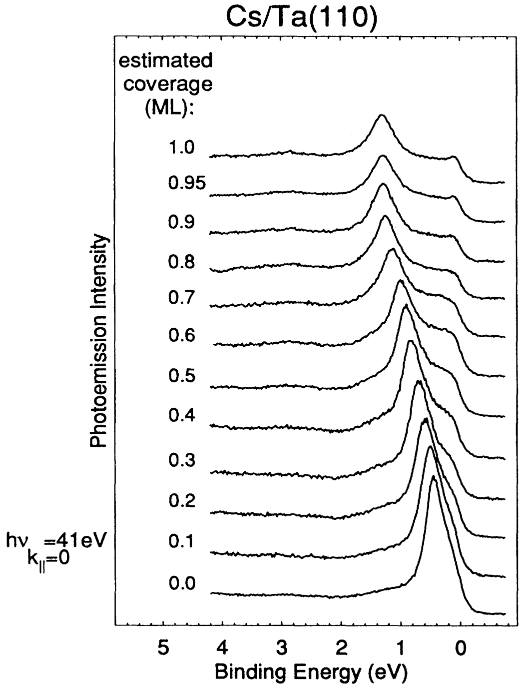

FIG. 7. Normal emission ARP spectra of cesium on Ta(110) as a function of coverage. Spectra were taken at room temperature. The clean Ta surface state at BE of 0.46 eV is continuously quenched and shifted to BE of 1.30 eV by monolayer coverage Cs.

nitude of the interaction should be larger for the lighter alkalis, driving the bonding level to higher binding energy.

In contrast to alkalis/Ta, the H/Ta system exhibits no dispersion nor intensity reduction of the modified surface state, even though the shift at zone center is nearly -2 eV. This demonstrates a striking difference between hydrogen and alkali chemisorption: with hydrogen, the surface state remains *d*-like and localized, while the alkali-modified state is substantially laterally delocalized by mixing with alkali *s* bands. The hydrogen atom is localized to one atomic substrate site, minimally affecting neighboring sites. The alkali atoms seem to affect the Ta surface band with substantial lateral range. This behavior can be partly explained by the spatial extent of the valence adatom *ns* levels relative to the substrate atomic spacing, which is larger for alkalis than for hydrogen. Perhaps more important is the location of the H 1*s* band well below the Fermi level, hybridizing negligibly with the Ta surface band.

Overlayer metallicity

Regardless of the mechanism behind the modification to the Ta surface state, it is clear that it has been substantially laterally delocalized, as evidenced by its acquired bandwidth. The state is still localized in the surface plane, since photon energy sweeps show no $k_{\perp}$ dispersion of the modified feature. Similar induced dispersions of *d*-type surface bands with alkali adsorption have been observed previously, but the effect is complicated by intrinsic surface band dispersion[14] or degeneracy with the bulk continuum.[15] In this study, the delocalization occurs continuously as a function of coverage. This is apparent in the smooth nature of the energy shift, effective mass, and quenching of the state at normal emission, and of the dispersion of the antibonding feature across E_F. Recent core-level measurements on the same sample similarly show no abrupt coverage-dependent behavior, and the authors conclude that strongly covalent alkali-substrate interactions occur at all coverages.[23] The absence of an abrupt transition to metallicity is not surprising. The alkali valence levels are so intermixed with metallic substrate bands that metallic behavior can be expected at all coverages.

An interesting contrast to the Ta(110) experiment is the study of Li/Be(1000).[8] The surface and bulk band structure for Be is quite different than for Ta, with classic nearly-free-electron behavior, yet similar surface band/alkali-*ns* hybridization is observed. A clear condensation transition is seen on Li/Be(1000), accompanied by the sudden appearance of the Li 2*s* band below the Fermi level. This can be interpreted as an overlayer nonmetal-metal transition, because the identity of the Li 2*s* band is still obvious. In fact, the Li 2*s* band exhibits different periodicity than the substrate SBZ. The hybridization of the Li 2*s* with the Be surface state is weak enough that overlayer and substrate states can still be distinguished. In this context, Be(1000) represents a "simple" metal surface. On Ta(110), the alkali-modified surface state cannot be called an overlayer band. While the modified band may be largely *s*-like at the center of the SBZ, it retains the character of the Ta surface band at larger $\mathbf{k}_{\|}$. Furthermore, the periodicity of the modified state is consistent with the Ta(110) SBZ. We cannot identify any electronic states specific to the alkali overlayer. The metallicity of the alkali overlayer on Ta(110) is collectively derived from partially occupied, strongly hybridized states common to both the surface Ta layer and the alkali layer. In principle, metallicity as a function of overlayer density can be linked to the coverage-dependent behavior of these states. Unfortunately, characterizing these states is much more difficult than for the case of an isolated overlayer state on simple metal substrates. There may be further interactions important to surface metallicity to which our experiment is insensitive. In particular, much of the alkali interaction with the substrate may involve the Ta bulk continuum. This would be difficult to identify because of level broadening and the relative weak photoemission cross section of *s*- and *p*-like features.

CONCLUSION

The Gurney model is inadequate to explain the adsorption of alkalis on Ta(011) because it isolates overlayer bands from the substrate. Rather than the ionization being determined solely by the occupation of the alkali *ns* resonance, charge transfer to the Ta substrate intimately involves the substrate valence *d* bands. This apparently occurs in such a way that the work-function behavior is very similar to less strongly hybridizing systems. The dipole layer which produces the work-function decrease is not derived only from the occupancy of valence bands, but also from their spatial distribution between the overlayer and substrate. The electronic structure near E_F varies substantially for different metals, and this should affect aspects of chemisorption other than the work function. This is especially true when comparing noble or NFE metals which have a smooth DOS and large dispersion, with transition metals that have a highly structured DOS due to localized *d*-like levels. We believe that strong interaction between overlayer and substrate states leads to substrate-mediated metallic behavior at very low coverages, preventing the abrupt overlayer condensation transition seen on simpler metal substrates.

ACKNOWLEDGMENTS

This work was carried out in part at the NSLS at Brookhaven National Laboratory, which is supported by the U.S. Department of Energy, Division of Materials Science and Division of Chemical Sciences. Financial support from the U.S. DOE under Grant No. DE-FG06-86-ER45275 is gratefully acknowledged. E.K. was supported by the DOE/NORCUS Fellowship Program. W.-K.C. would like to thank the Rotary Foundation for financial support.

---

[1] R. W. Gurney, Phys. Rev. **47**, 479 (1935).
[2] N. D. Lang, Phys. Rev. B **4**, 4234 (1972).
[3] J. P. Muscat and D. M. Newns, Surf. Sci. **74**, 355 (1978).
[4] M. Scheffler, Ch. Droste, A. Fleszar, F. Maca, G. Wachutka, and G. Barzel, Physica B **172**, 143 (1991).
[5] E. W. Plummer and P. A. Dowben, Prog. Surf. Sci. **42**, 201 (1993).
[6] B. Woratschek, W. Sesselmann, J. Kuppers, G. Ertl, and H. Haberland, Phys. Rev. Lett. **55**, 1231 (1985).
[7] K. Horn, A. Hohlfeld, J. Somers, Th. Lindner, P. Hollins, and A. Bradshaw, Phys. Rev. Lett. **61**, 2488 (1988).
[8] G. M. Watson, P. A. Bruhwiler, E. W. Plummer, H.-J. Sagner, and K.-H. Frank, Phys. Rev. Lett. **65**, 468 (1990); G. M. Watson, P. A. Bruhwiler, H.-J. Sagner, K.-H. Frank, and E. W. Plummer, Phys. Rev. B **50**, 17 678 (1994).
[9] H. B. Nielsen, U. Burghaus, G. Brostrom, and E. Matthias, Surf. Sci. Lett. **234**, L271 (1990).
[10] J. Neugebauer and M. Scheffler, Phys. Rev. Lett. **71**, 577 (1993).
[11] N. Mott, *Metal-Insulator Transitions* (Taylor & Francis, London, 1990).
[12] H. Ishida, Phys. Rev. B **40**, 1341 (1989).
[13] H. Ishida, Phys. Rev. B **42**, 10 899 (1990).
[14] P. Soukiassian, R. Riwan, J. Lecante, E. Wimmer, S. R. Chubb, and A. J. Freeman, Phys. Rev. B **31**, 4911 (1985).
[15] J. Cousty and R. Riwan, Europhys. Lett. **3**, 1119 (1987).
[16] E. Wimmer, A. J. Freeman, J. R. Hiskes, and A. M. Karo, Phys. Rev. B **28**, 3074 (1983).
[17] E. Kneedler, K. E. Smith, D. Skelton, and S. D. Kevan, Phys. Rev. B **44**, 8233 (1991).
[18] M. Blaszczyszyn, Surf. Sci. **59**, 533 (1976).
[19] D. L. Fehrs and R. E. Stickney, Surf. Sci. **24**, 309 (1971).
[20] E. Kneedler, Ph.D. thesis, University of Oregon, 1994.
[21] W. A. Harrison, *Electronic Structure and the Properties of Solids* (Freeman, San Francisco, 1980).
[22] A. R. Bishop and A. Mookerjee, J. Phys. C **7**, 2165 (1974); S. S. A. Razee, S. S. Rajput, R. Prasad, and A. Mookerjee, Phys. Rev. B **42**, 9361 (1990).
[23] A. B. Andrews, D. M. Riffe, and G. K. Wertheim, Phys. Rev. B **49**, 8396 (1994).